Weiyi Lu[a], Taewan Kim[b], Cang Zhao[a], Yu Qiao[a,b]
[a] University of California – San Diego, Department of Structural Engineering, La Jolla, USA
[b] University of California – San Diego, Program of Materials Science & Engineering, La Jolla, USA

Effects of molecular polarity on nanofluidic behavior in a silicalite

While "like attracts like" is common sense for large surfaces, here we show that in a nanopore the effective solid–liquid interfacial tension can be quite independent of the liquid polartiy. Moreover, as the liquid molecules and ions are confined, their behavior can be either reversible or irreversible, depending on the liquid composition. These unique phenomena can be attributed to the confinement effects and the absence of bulk liquid phase in the nanoenvironment.

Keywords: Polarity; Nanopore; Interfacial tension

1. Introduction

According to conventional surface theory, e. g. [1] the polarities of the solid surface and the liquid molecules dominate the wettability of a solid–liquid interface. For instance, a polar solid surface is usually wettable to a polar liquid (e. g. water), and would be nonwettable to a nonpolar liquid (e. g. an oil). This understanding, sometimes referred to as "like attracts like", is fundamental to studies on surface and interface phenomena, e. g. surfactants, surface coating, interface properties, among others.

In the past few decades, with the development of nanoporous materials, solid–liquid interactions in confining nanoenvironments have received increasing attention. Nanoporous materials, such as zeolites, silica gels, etc., are solids containing large volume fractions of nanometer (nm) sized pores. These nanopores can be either isolated or interconnected, and the nanopore size is typically 0.6–100 nm [2]. The porosity ranges from 15 % to 85 % [3]. They are usually synthesized via templating techniques. As both template and network agents are used, the template molecules are first precipitated and then removed by combustion or extraction [4]. Nanoporous materials are widely used for catalysis, mixture separation, absorption and adsorption, among others [5–7]. Both experimental and computer simulation results indicate that the gas phase effects, which are often negligible at large solid surfaces, can be significant in a nanotube or nanochannel [8]. More importantly, the solid–liquid interactions are strongly confined by the nanopore walls [9, 10]. For instance, under certain conditions, even for nominally wettable nanopore surfaces a relatively large pressure must be applied so as to trigger liquid infiltration, and there should be sufficient space for a "free volume" a few times larger than the sizes of liquid molecules [11, 12].

Currently, not only theoretical analyses but also basic experimental observations in this area are incomplete. Particularly, the effect of polarity of the liquid phase has not been systematically examined.

2. Experimental

In the current study, we investigated a compressible solid–liquid nanohybrid (CSLN). The CSLN was produced by suspending 0.5 g of silicalite-1 crystals in 7 ml of liquid and sealing it in a stainless steel cylinder, as depicted in Fig. 1. The silicalite-1 was synthesized via a sol treatment method. The sol contained 1 part of SiO_2, 0.08 parts of tetrapropylammonium bromide (TPABr), 1 part of NH_4F, and 20 parts of H_2O (molar composition). First, 10.42 g of tetraethoxysilane (TEOS) was added as the silicon source into a polypropylene (PP) container with 1.07 g of TPABr and 9.00 g of deionized water. The mixture was stirred vigorously at room temperature for 0.5 h so that the TEOS was hydrolyzed, until the solution became single-phased. Then, an NH_4F solution (1.90 g of NH_4F in 9.00 g of deionized water) was injected into the container. After the mixture was continuously stirred for 1 h at room temperature, the reactant was sealed in a stainless steel autoclave and hydrothermally treated at 200 °C for 2 days. The material was then washed with cold deionized water, filtered by a Buchner funnel with Whatman filter paper, and finally calcined in a tube furnace at 550 °C for 2 h. During the calcination process, an air flow was maintained to remove the organic template. The synthesized silicalite-1 crystals were characterized by means of X-ray diffraction (XRD) (Fig. 2) as well as gas absorption analysis. The nanopore size was 0.6 nm; the specific nanopore surface area was 400 $m^2\ g^{-1}$; and the specific nanopore volume was 0.2 $cm^3\ g^{-1}$.

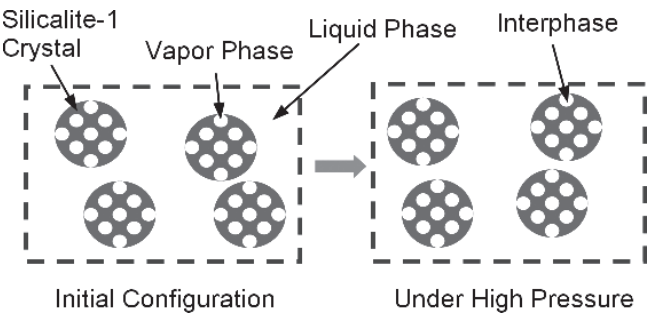

Fig. 1. Schematic of pressure induced interphase formation.

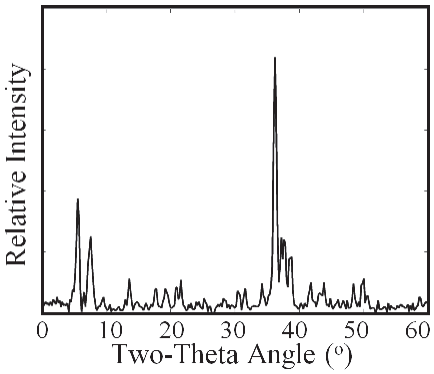

Fig. 2. Characteristic XRD peaks of the silicalite-1 showing the crystalized structures of the material.

The cross-sectional diameter of the cylinder was 9.5 mm. The liquid phase was either deionized water (H_2O), diethyl ether ($CH_3CH_2OCH_2CH_3$), or 3 wt.% aqueous solution of ammonia ($NH_3 \cdot H_2O$). Water molecules are highly polar; diethyl ether molecules are non-polar; and ammonia solution is ionic. They are either neutral or basic, and, thus, do not change the nanopore surface structures. By using an Instron machine, a piston was compressed into the cylinder. The loading rate was 0.5 mm min^{-1}. As the inner pressure reached 120 MPa, the piston was moved out at the same speed. Typical sorption isotherm curves are shown in Fig. 3.

3. Results and discussion

The XRD result shown in Fig. 2 indicates clearly that the silicalite-1 is well crystallized [13]. It contains two sets of nanopores. One set is straight, and the other is of a zigzag structure [14]. The nanopores are interconnected, forming a three-dimensional network [15]. Because the silica/alumina ratio is high, the defect density at inner surfaces of nanopores is low, and, therefore, the degree of hydrophobicity is high. As a result, in a water based CSLN, under ambient pressure the H_2O molecules cannot enter the nanopores. In the framework of conventional continuum fluid mechanics, the critical infiltration pressure of a liquid in a lyophobic channel is determined by the contact angle, θ. In a nanopore of silicalite-1, since across the cross-section the space is sufficient for only 1–2 liquid molecules, θ cannot be defined. Nevertheless, as a first-order approximation, the external work and the interfacial energy can be assessed as $p(\pi r^2)L$ and $\Delta\gamma \cdot (2\pi r)L$, respectively; thus, $\Delta\gamma = p \cdot r/2$, where $\Delta\gamma$ is the increase in effective interfacial tension, p is the external pressure, r is the effective nanopore size, and L is the depth of liquid infiltration. That is, as $p = 2 \cdot \Delta\gamma/r$, a liquid molecule inside a nanopore is neutrally stable. In a previous work [15], it was argued that it is more appropriate to analyze the infiltration of liquid molecules in nanopores in the context of effective phase transformation. The liquid outside the nanopores can be regarded as the bulk phase; the liquid inside the nanopores can be regarded as the interphase. The interphase is strongly affected by the surrounding nanopore walls. If the nanopore size is smaller than the van der Waals distance and the Debye length, the ordinary interface layer and solvated structure cannot be formed. Note that in the above discussion the important influence of the pore configuration is ignored. In a real pore, the critical pressure of the interphase formation can be more dependent on the effective liquid–vapor interface tension, the details of which will form a part of our future study.

In a molecular sized nanopore, the interphase can be of a chain-like structure [16]. If the nanopore size is a few times larger than the liquid molecule, the interphase structure is less ordered [17]. If the nanopore size is more than an order of magnitude larger than the liquid molecule, the interphase consists of an interface layer and a bulk phase, which converges to the prediction of continuum theory [18, 19]. As the pressure reaches the critical value, p_{cr}, pressure induced interphase formation takes place. Extensive mass and energy exchanges occur among the liquid, gas, and solid phases in nanopores. As the interphase is formed, the volume of bulk liquid phase outside the nanopores is reduced, and, thus, a plateau region is observed in the sorption isotherm curve (Fig. 3). The width of the plateau indicates the effective pore volume involved in the interphase formation process.

If the liquid phase is H_2O, $p_{cr} = 94.3$ MPa. For self-comparison purpose, in this article p_{cr} is defined as the pressure at the onset of the plateau region where the slope of sorption isotherm curve is reduced by 50%. As the interphase formation continues, even though the silicalite-1 is well crystallized and the nanopore size is uniform, the critical pressure keeps increasing, due to the "internal friction" associated with the interphase growth. The width of the plateau region is about 0.1 $cm^3\ g^{-1}$, smaller than the measured specific nanopore volume, probably because of the effective van der Waals distance between the confined liquid molecules and the nanopore wall [20, 21]. The effective van der Waals distance is about 0.1 nm, smaller than the theoretical prediction, which may be attributed to the irregular chain-like liquid molecular configuration [22]; that is, the liquid molecules are not well aligned, because of the thermal motion as well as the zig-zag nanopore structure. The effective interfacial tension is 16.5 mJ m^{-2}, typical for a polar liquid at a large surface, e. g. a flat silica surface [23].

As the interphase formation ceases, the volume of bulk liquid phase decreases only slightly as the pressure further increases, and the system becomes nearly incompressible. When the external load is reduced, as the pressure is relatively high, the interphase is stable. When p is slightly low-

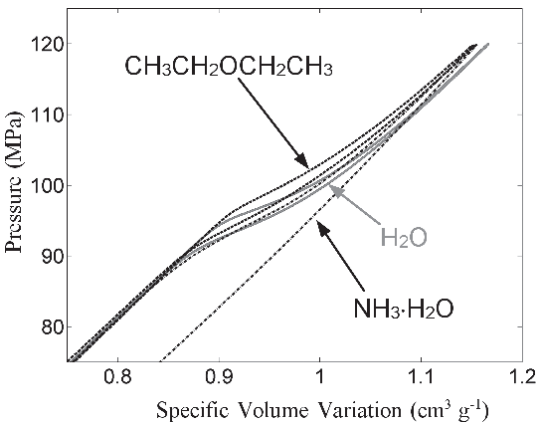

Fig. 3. Typical sorption isotherm curves.

er than p_{cr} by about 2 %, the interphase begins to decompose. The volumes of the empty nanopores (the vapor phase) and the bulk liquid phase increase, forming another plateau region in the sorption isotherm curve. Since the profiles of the loading and unloading paths are quite similar to each other, the motion of liquid molecules into and out of nanopores is reversible, suggesting that the lattice resistance is small. Note that the slope of the plateau region is about 80 MPa · g cm^{-3}, which should be related to the long-range interaction [24]. The nanopore depth associated with the interphase formation can be taken as the crystal size, around 20 μm. Thus, the effective pressure gradient in the interphase is approximately 0.5 MPa μm^{-1}, or, if the liquid molecular size is taken as 0.2 nm, 4×10^{-18} N per molecule.

As the liquid phase is changed to diethyl ether, as shown in Fig. 3, most of the characteristics of the sorption isotherm discussed above remain the same, except that the system volume variation is reduced by nearly 20 %. The change in system volume may be associated with the difference in molecular size. Since diethyl ether molecules are larger than water molecules, especially along the axial direction, their structures inside nanopores can be more regular, and, consequently, the effective van der Waals distance to the nanopore wall is larger, resulting in the relatively small volume variation of the bulk liquid phase.

An interesting phenomenon is that, although water molecules are highly polar and diethyl ether molecules are nonpolar, the critical infiltration pressures are nearly the same, as shown in Table 1. The effective solid–liquid interfacial tensions are similar to each other; the difference is only 1 %, within the tolerance of the testing machine. This is contradictory to the predictions of conventional interface theories. Since the negatively charged defect sites at nanopore walls are removed by increasing the silica content, the surface is nonpolar. At the macroscopic scale, such a solid surface should be wettable to a nonpolar liquid, such as diethyl ether. Clearly, in the current investigation, the energy barrier for the liquid molecules to enter the nanopore is independent of the degree of polarity. In a nanopore, due to the confinement effect of surrounding solid surface, the ordinary interface layer breaks down. It is likely that the liquid molecules are aligned in a chain-like line [25]. Along the radius direction, the liquid molecules are subjected to quasi-isotropic forces from the network. Even though the solid–liquid interaction force is attractive, i. e. the nanopore surface is nominally wettable, as the equilibrium solid–liquid distance is disturbed, an external work still needs to be done to "squeeze" the liquid molecules in the confining nanoenvironment. This is compatible with the experimental observation [11, 26, 27] that if the liquid phase is a benzene based nonpolar chemical, no interphase can be formed even when the pressure is increased to 500 MPa, since the cross-sectional diameter of benzene molecule is quite large. Because the solid–liquid interaction is insensitive to the degree of polarity, the unloading behaviors of water and diethyl ether are also similar.

If the liquid phase is an aqueous solution of ammonia, as shown in Fig. 3, the interphase becomes much more stable. While the loading part of the sorption isotherm curve is similar to that of water and diethyl ether, as the pressure is reduced no significant system volume increase can be detected. Clearly, as the liquid becomes ionic, the energy well confining the interphase molecules and ions is much larger, and, therefore, the confined molecules and ions are "locked" inside the nanopores even when the external pressure is removed. The increase in energy well is reflected by the relatively large slope of the plateau region in the sorption isotherm curve, i. e. a larger internal friction needs to be overcome to form the interphase. With the higher energy barrier, the effect of thermal motion is less pronounced and the system behavior is hysteretic.

4. Concluding remarks

In summary, the behavior of pressurized polar, nonpolar, and electrolyte solution in nanopores of a silicalite-1 has been investigated experimentally. The effective solid–liquid interfacial tension in the nanoenvironment is independent of the liquid polarity, which is against the conventional understanding of "like attracts like". For the two neat liquids under investigation, the lattice resistance is insufficient to confine liquid molecules, and, thus, the interphase formation and decomposition is nearly reversible. For the electrolyte solution, the lattice resistance can be much larger and the interphase is stable even when the external pressure is removed. The current investigation is focused on only one type of nanoporous material. The liquid/solid properties and nanopore configurations must be varied in broader ranges to reach more general conclusions.

This work was supported by The National Science Foundation under Grant No. ECCS-1028010.

References

[1] C.J. van Oss: Interfacial Forces in Aqueous Media, CRC Press, Boca Raton (2006). DOI:10.1201/9781420015768
[2] S. Polarz, B.J. Smarsly: Nanosci. Nanotech. 2 (2002) 581. DOI:10.1166/jnn.2002.151
[3] R.M.A. Roque-Malherbe: Adsorption and Diffusion in Nanoporous Materials. CRC Press, Boca Raton (2007). DOI:10.1201/9781420046762
[4] G.Q. Lu, X.S. Zhao: Nanoporous Materials – Science and Engineering. Imperial College Press, London (2005).
[5] N.Z. Logar, V. Kaucic: Acta Chim. Slovenica. 53 (2006) 117.
[6] V. Castelvetro, C. De Vita: Adv. Colloid Interface Sci. 108 (2004) 167. PMid:15072940; DOI:10.1016/j.cis.2003.10.017

Table 1. Measurement results of system performance.

Liquid Phase	Pressure of Interphase Formation, p_{cr} (MPa)	Hysteresis in Pressure (MPa)	Specific Volume Variation (mm^3 g^{-1})	Effective Interface Tension (mJ m^{-2})
H_2O	94.3	2.1	105	16.5
$CH_3CH_2OCH_2CH_3$	95.6	2.3	81	16.7
$NH_3 \cdot H_2O$	91.1	91.1	92	15.9

[7] M.A. Hillmyer: Block Copolym. II Adv. Polym. Sci. 190 (2005) 137. DOI:10.1007/12_002
[8] Y. Qiao, G. Cao, X. Chen: J. Am. Chem. Soc. 129 (2007) 2355. PMid:17279750; DOI:10.1021/ja067185f
[9] R.Z. Wan, J.Y. Li, H.J. Lu, H.P. Fang: J. Am. Chem. Soc. 127 (2005) 7166. PMid:15884958; DOI:10.1021/ja050044d
[10] M. Majumder, N. Chopra, R. Andrews, B.J. Hinds: Nature 438 (2005) 44. PMid:16267546; DOI:10.1038/438044a
[11] A. Han, Y. Qiao: J. Am. Chem. Soc. 128 (2006) 10348. PMid:16895383; DOI:10.1021/ja062037a
[12] F.B. Surani, X. Kong, Y. Qiao: Appl. Phys. Lett. 87 (2005) 163111. DOI:10.1063/1.2106002
[13] S. Bhatia: Zeolite Catalysts – Principles and Applications. CRC Press, Boca Raton (1989).
[14] S.M. Auerbach, K.A. Carrado, P.K. Dutta: Handbook of Zeolite Science and Technology. CRC Press, Boca Raton (2003). DOI:10.1201/9780203911167
[15] A. Han, X. Kong, Y. Qiao: J. Appl. Phys. 100 (2006) 014308. DOI:10.1063/1.2214368
[16] D.T. Wasan, A.D. Nikolov: Nature 423 (2002) 156. PMid:12736681; DOI:10.1038/nature01591
[17] N.Y. Chen, T.F. Degnan, C.M. Smith: Molecular Transport and Reaction in Zeolite. Wiley-VCH, New York (1994).
[18] C. Degueldre, A. Scholtis, A. Laube, M.J. Turrero, B. Thomas: Appl. Geochem. 18 (2003) 55. DOI:10.1016/S0883-2927(02)00048-3
[19] R. Kimmich: Chem. Phys. 284 (2002) 253. DOI:10.1016/S0301-0104(02)00552-9
[20] G.M. Wang, A.C. Sandberg: Nanotech. 18 (2007) 135702. PMid:21730387; DOI:10.1088/0957-4484/18/13/135702
[21] N.R. de Souza, A.I. Kolesnikov, C.J. Burnham, C.K. Loong: J. Phys. – Condens. Mat. 18 (2006) S2321.
[22] S.R. Vogel, M.M. Kappes, F. Hennrich, C. Richert: Chem. – Eur. J. 13 (2007) 1815. PMid:17133636; DOI:10.1002/chem.200600988
[23] S. Hartland: Surface and Interface Tension. CRC Press, Boca Raton (2004). DOI:10.1201/9780203021262
[24] R.H. French, V.A. Parsegian, R. Podgornik, R.F. Rajter, A. Jagota, J. Luo, D. Asthagiri, M.K. Chaudhury, Y.M. Chiang, S. Granick, S. Kalinin, M. Kardar, R. Kjellander, D.C. Langreth, J. Lewis, S. Lustig, D. Wesolowski, J.S. Wettlaufer, W.Y. Ching, M. Finnis, F. Houlihan, O.A. von Lilienfeld, C.J. van Oss, T. Zemb: Rev. Modern Phys. 82 (2010) 1887. DOI:10.1103/RevModPhys.82.1887
[25] M. Whitby, N. Quirke: Nature Nanotech. 2 (2007) 87. PMid:18654225; DOI:10.1038/nnano.2006.175
[26] F.B. Surani, X. Kong, Y. Qiao: Appl. Phys. Lett. 87 (2005) 251906. DOI:10.1063/1.2106002
[27] A. Han, X. Kong, Y. Qiao: J. Phys. D. Appl. Phys. 40 (2007) 3436. DOI:10.1088/0022-3727/40/11/026

(Received June 4, 2012; accepted September 19, 2012; online since November 22, 2012)

Bibliography

DOI 10.3139/146.110900
Int. J. Mater. Res. (formerly Z. Metallkd.)
104 (2013) 6; page 594 – 597

ISSN 1862-5282

Correspondence address

Professor Yu Qiao
9500 Gilman Drive
La Jolla
CA 92093-0085
USA
Tel.: +1-858-534-3388
Fax: +1-858-534-1310
E-mail: yqiao@ucsd.edu

You will find the article and additional material by entering the document number **MK110900** on our website at *www.ijmr.de*